

# Spontaneous and Stimulated Raman Scattering from Surface Phonon Modes in Aggregated SiO<sub>2</sub> Nanoparticles

Yu. D. Glinka<sup>\*,†,‡</sup> and M. Jaroniec<sup>†</sup>

Separation and Surface Science Center, Department of Chemistry, Kent State University, Kent, Ohio 44242,  
and Institute of Surface Chemistry of the National Academy of Sciences of Ukraine, prospekt Nauki 31,  
Kiev 252650, Ukraine

Received: June 4, 1997<sup>®</sup>

A spontaneous and stimulated Raman scattering from the surface phonon modes (SPMs) in aggregated amorphous silica (SiO<sub>2</sub>) nanoparticles is reported for the first time. The SPMs are located between Raman peaks corresponding to the amorphous silica bulk transverse-optical (TO) and longitudinal-optical (LO) bending phonon modes. An anomalously large TO–LO splitting ( $\sim 185\text{ cm}^{-1}$ ) of bending modes for bulk amorphous silica was observed. Six different SPMs corresponding to elliptical nanoparticles in two mediums of different effective dielectric constants were detected by the spontaneous Raman scattering spectra. One can obtain a good agreement with the theory for SPMs by assuming the anomalously large TO–LO splitting of bending modes in nanoparticles of the amorphous SiO<sub>2</sub>. The stimulated Raman scattering from SPMs was observed under second harmonic excitation of the YAG:Nd pulsed laser. The threshold value was estimated as  $\sim 60\text{ MW cm}^{-2}$ .

## Introduction

One of the fundamental problems of modern solid-state physics is the understanding of the nature of interactions in small particles of nanometer size. The study of such objects allows one to form a bridge between physics of free molecules and condensed matter. Semiconducting nanoparticles embedded in a dielectric matrix (quantum dots),<sup>1–5</sup> fullerenes,<sup>6,7</sup> carbon nanotubes,<sup>7–11</sup> finite diatomic ionic crystals,<sup>12,13</sup> silicon nanoclusters,<sup>14,15</sup> and silica nanoparticles<sup>16,17</sup> have recently received considerable attention. The study of vibrational properties of nanoparticles is important for addressing the aforementioned problem.<sup>6–13,15</sup> Effects of a finite solid size on optical phonons have been investigated extensively by IR absorption measurements. For different ionic microcrystals new absorption bands were observed. These bands were assigned to surface phonon modes (SPMs) and interpreted successfully by electromagnetic theories.<sup>18</sup> The theory of the SPM excitation for particles of many common insulators was considered elsewhere<sup>12</sup> by assuming differences in their shape, orientation, and surrounding mediums. Also, some theoretical discussion of the Raman scattering from SPMs was presented.<sup>18,19</sup> In contrast, there are not many experimental works on the Raman scattering from SPMs in small solid particles,<sup>13,20</sup> because a correct identification of these modes from numerous peaks of Raman spectra is difficult. From a theoretical viewpoint,<sup>18</sup> the Raman peak corresponding to the SPM should satisfy the following requirements: (i) its intensity should increase as the particle size decreases, (ii) it should be located between the bulk transverse-optical (TO) and longitudinal-optical (LO) phonon frequencies, and (iii) it should shift to lower frequencies as the dielectric constant of the surrounding medium increases.

In the current work, the spontaneous and stimulated Raman scattering from the SPMs of amorphous silica (SiO<sub>2</sub>) nanoparticles smaller than the excitation wavelength (514.5 and 532

nm) and aggregated into micrometer size clusters (globules) is utilized to determine the shape of these particles. It is known<sup>12</sup> that the SPM excitation can occur only for particles much smaller than the excitation wavelength. Evidently the above-mentioned nonstrong condition to the primary particle size does not permit the use of this method for size-selective measurements.

Since silica particles are amorphous (i.e., isotropic medium), Raman peaks related to the one-phonon scattering should be depolarized. In contrast, for Raman peaks related to SPMs the depolarization ratio ( $I_{\perp}/I_{\parallel}$ , where  $I_{\perp}$  and  $I_{\parallel}$  are the Raman peak intensities recorded respectively for perpendicular and parallel geometries with respect to the laser beam polarization) can be smaller than unity. This results from the fact that in the case of the elliptical particles the polarization along each axis of the ellipsoid is different. Therefore, in addition to above-mentioned three requirements the Raman peaks related to SPMs should be particularly polarized. In the current study of amorphous silica nanoparticles, several new peaks in the spontaneous Raman spectra ( $\lambda_{\text{exc}} = 514.5\text{ nm}$ ) were found in addition to the spectrum of the bulk vitreous SiO<sub>2</sub>. These peaks were assigned to SPMs. The stimulated Raman scattering (SRS) for these modes was measured by using the intense pulsed laser excitation ( $\lambda_{\text{exc}} = 532\text{ nm}$ ).

## Experimental Section

The samples were prepared by the following technique. The disperse silicon dioxide (aerosil) of the specific surface area of  $160\text{ m}^2\text{ g}^{-1}$  (the average diameter of primary particles is  $\sim 40\text{ nm}$ )<sup>21</sup> was heated in air at different temperatures in the range of  $T_{\text{h.t.}} = 30\text{--}1000\text{ }^{\circ}\text{C}$  for 2 h and compacted under a pressure of  $4.0 \times 10^5\text{ N m}^{-2}$ . Raman measurements were carried out by using a conventional 90° scattering geometry. The spontaneous Raman scattering spectra were excited by the 514.5-nm line of an Ar-ion laser and recorded in the Stokes region by a double monochromator and photon-counting system. To investigate polarization properties, the spectra at  $X(\text{ZZ})Y$  and  $X(\text{ZX})Y$  geometries ( $I_{\parallel}$  and  $I_{\perp}$ , respectively) were measured, where the  $X$  axis is taken for the direction of the laser beam with its electric

\* To whom correspondence should be addressed.

<sup>†</sup> Kent State University.

<sup>‡</sup> Institute of Surface Chemistry of the National Academy of Sciences of Ukraine.

<sup>®</sup> Abstract published in *Advance ACS Abstracts*, October 1, 1997.

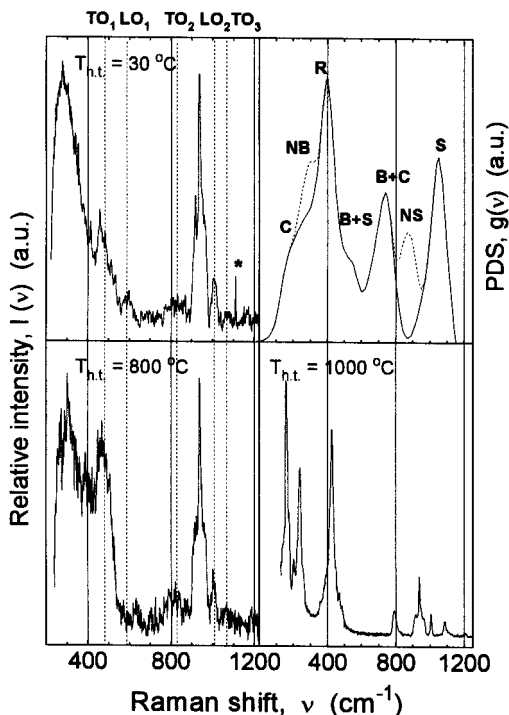


**Figure 1.** Raman spectra of the disperse silica treated at different temperatures  $T_{h.t.}$ . The phonon density of states (PDS) for the vitreous  $\text{SiO}_2$  is shown in upper right section.<sup>27</sup> Capital letters denote the following vibrations of the Si–O–Si bond: C, silicon; B, oxygen bending; R, oxygen rocking; S, oxygen symmetric stretch; N, NBOA.

vector in the  $Z$  direction and the  $Y$  axis showing the direction of scattered light. The registration system was protected against Ar-plasma lines radiation. In the case of the stimulated Raman scattering, spectra were excited by the second harmonic of the amplified Nd:YAG pulsed laser ( $\lambda_{\text{exc}} = 532 \text{ nm}$ ,  $I_L = 10^6\text{--}10^8 \text{ W cm}^{-2}$ ,  $\tau_p = 20 \text{ ns}$ ) and recorded also in the Stokes region by a single monochromator. All measurements were performed at room temperature in air.

## Results and Discussion

Spontaneous Raman spectra of the disperse silica samples pretreated at different temperatures are shown in Figure 1. The general view of the Raman spectra for the samples treated at  $T_{h.t.} = 30 \text{ °C}$  roughly corresponds to typical spectra of the vitreous silica<sup>22</sup> except for the group of narrow peaks in the region of  $900\text{--}990 \text{ cm}^{-1}$  and a single narrow peak at  $1110 \text{ cm}^{-1}$  (last peak is marked by a star). It is well-known<sup>23,24</sup> that there are three local vibrational motions of rocking, bending, and asymmetrical stretching of oxygen atoms with respect to the silicon atom pairs. On the other hand, in terms of the classical optical-dispersion theory, each vibrational motion is characterized by an independent harmonic electric-dipole oscillator with the corresponding strength and density of the TO and LO modes ( $\text{TO}_1\text{--LO}_1$ ,  $\text{TO}_2\text{--LO}_2$ ,  $\text{TO}_3\text{--LO}_3$  pairs, respectively).<sup>25</sup> Three well-known transverse-optical modes of the Si–O–Si groups, identified as  $\text{TO}_1 \sim 460$ ,  $\text{TO}_2 \sim 800$ , and  $\text{TO}_3 \sim 1070 \text{ cm}^{-1}$ , were reported previously for the amorphous silica.<sup>22,23,25</sup> The broad Raman peaks reported in the current work, which are positioned at  $\sim 460$ ,  $\sim 820$ , and  $\sim 1070 \text{ cm}^{-1}$ , correspond to these vibrational modes, respectively. Also, it is interesting to compare the experimental frequencies of Raman peaks with the phonon density of states (PDS) for the vitreous  $\text{SiO}_2$  that were obtained by using coherent inelastic neutron scattering<sup>26</sup> and theoretical calculations.<sup>27</sup> So, the  $820 \text{ cm}^{-1}$  peak and the peak at  $\sim 300 \text{ cm}^{-1}$  can be assigned to the vibrations of nonbridging

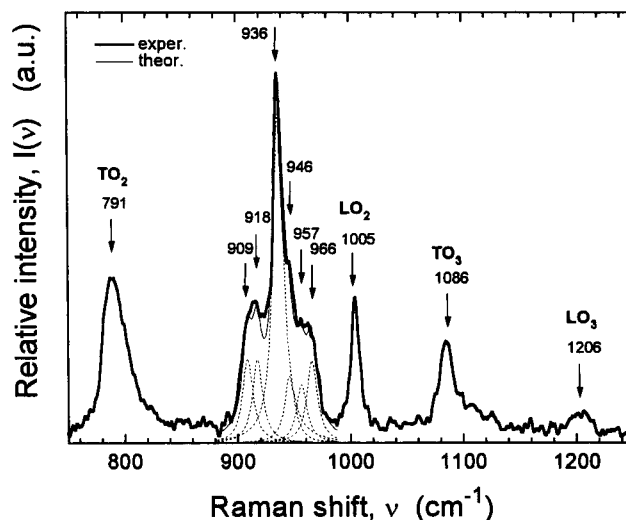


**Figure 2.** Part of the Raman spectrum of the disperse silica prepared at  $T_{h.t.} = 1000 \text{ °C}$ . A theoretical representation of SPMs is shown. Lorentz profiles corresponding to different SPMs are drawn by dashed lines. The phonon modes of  $\alpha$ -quartz are indicated by capital letters.

oxygen atoms (NBOA) (Figure 1). Since the disperse silicon dioxide prepared at temperatures up to  $600 \text{ °C}$  contains the surface OH groups in abundance,<sup>28</sup> one can assume that these frequencies correspond to the oxygen motions of symmetrical and bending vibrations of oxygen present in hydroxyl groups.

The LO modes, which are normally infrared inactive, in Raman spectra of the disperse  $\text{SiO}_2$  appear as weak peaks, which is in agreement with measurements of the vitreous silica.<sup>22</sup> The peak at  $590 \text{ cm}^{-1}$  can be assigned to the  $\text{LO}_1$  mode and the  $1005 \text{ cm}^{-1}$  peak to the  $\text{LO}_2$  mode. The  $\text{LO}_3$  mode and modes that are commonly assigned to the disorder-induced vibrational coupling effect ( $\text{TO}_4\text{--LO}_4$ )<sup>23,25</sup> appear as weak peaks (region of  $1100\text{--}1300 \text{ cm}^{-1}$ ) and will not be considered. Note that the  $\text{LO}_2$  mode peak at  $1005 \text{ cm}^{-1}$  was observed for the first time. Since from the general viewpoint the splitting of the TO–LO-phonon frequencies is determined by the local electric field, one can suggest that an anomalously large splitting of  $\text{TO}_2\text{--LO}_2$  modes ( $\sim 185 \text{ cm}^{-1}$ ; this value for the bulk  $\alpha$ -quartz is about  $15 \text{ cm}^{-1}$ )<sup>29</sup> in  $\text{SiO}_2$  nanoparticles results from the high local electric field. This results from the fact that the bending vibrations of the oxygen atom in hydroxyl groups (or NBOA) and the bending vibrations of these atoms in different  $\text{SiO}_4$  tetrahedra interact very strongly so that these modes have an extended, delocalized character.<sup>24</sup> It seems reasonable to say that this phenomenon is a common property for small particles and thin films.

The formation of the bulk crystalline structure from small amorphous  $\text{SiO}_2$  particles occurs at  $T_{h.t.} \sim 1000 \text{ °C}$ . All Raman peaks are narrowed and can be assigned to typical vibrations of  $\alpha$ -quartz.<sup>29</sup> The  $\alpha$ -quartz bulk vibrational modes are positioned at  $\text{TO}_1 \sim 424$ ,  $\text{LO}_1 \sim 471$ ,  $\text{TO}_2 \sim 791$ ,  $\text{LO}_2 \sim 1005$ ,  $\text{TO}_3 \sim 1086$ , and  $\text{LO}_3 \sim 1206 \text{ cm}^{-1}$  (Figure 2).

For silica nanoparticles new Raman peaks were observed in addition to those for the bulk vitreous  $\text{SiO}_2$ . These bands are located at  $\sim 917$ ,  $\sim 936$ , and  $\sim 964 \text{ cm}^{-1}$  and characterized by the splitting of peaks in two components. The position of these peaks is between the  $\text{TO}_2$  and  $\text{LO}_2$  phonon frequencies and practically does not change by heat pretreatment of samples, whereas their width slightly decreases ( $\sim 3 \text{ cm}^{-1}$ ) with increasing pretreatment temperature. Note also that the intensities of these peaks drastically decrease in comparison to the  $\alpha$ -quartz bulk vibrational modes when the pretreatment temperature corresponds to the bulk crystalline phase formation (Figure 1). One

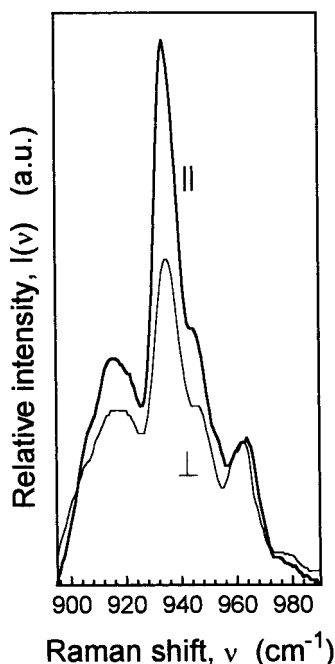


**Figure 3.** Part of Raman spectra corresponding to SPMs for the sample prepared at  $T_{\text{h.t.}} = 600$  °C. Different geometries of the measurement are shown.

of three peaks,  $964\text{ cm}^{-1}$  is depolarized, whereas two others have the depolarization ratio less than unity:  $I_{\perp}/I_{\parallel} = 0.87$  (for the  $917\text{ cm}^{-1}$  peak) and  $I_{\perp}/I_{\parallel} = 0.69$  (for the  $936\text{ cm}^{-1}$  peak) (Figure 3). The combination of all these facts allows one to assume that the peaks located at  $\sim 917$ ,  $936$ , and  $964\text{ cm}^{-1}$  are due to SPMs.

The single narrow peak at  $1110\text{ cm}^{-1}$  lies between the  $\text{TO}_3$  and  $\text{LO}_3$  phonon frequencies (Figure 1) and also can be assigned to the SPM. This peak broadened with increasing pretreatment temperature up to  $600$  °C and then vanished. Note that the same IR absorption peak located at  $1111\text{ cm}^{-1}$  was observed early for small amorphous quartz spheres in the KBr matrix.<sup>12</sup> Therefore, one can conclude that a small concentration of spherical particles is present in the initial sample, but after heat pretreatment the shape of particles becomes elliptical.

In the case of the intense pulsed laser excitation ( $\lambda_{\text{exc}} = 532\text{ nm}$ ), one can observe the SRS for these modes (Figure 4). The SRS peak is located at  $\sim 559.8\text{ nm}$ , which corresponds to the Stokes line of the  $935\text{ cm}^{-1}$  Raman shift. The threshold value of the laser intensity is estimated as  $\sim 60\text{ MW cm}^{-2}$ . The laser intensity dependence of the SRS peak intensity ( $I_s$ ) can be sufficiently well described by an exponent function (Figure 4).

As noted above, the frequencies that correspond to SPMs must lie between  $\nu_{\text{TO}}$  and  $\nu_{\text{LO}}$ . It is known<sup>12</sup> that the SPM frequencies satisfy the following condition

$$\nu_{\text{SPM}(k)}^2 = \nu_{\text{TO}}^2 \frac{\epsilon_0 + \epsilon_m (1/L_k - 1)}{\epsilon_{\infty} + \epsilon_m (1/L_k - 1)} \quad (1)$$

where  $\epsilon_0$  is the static dielectric constant of the specimen (for amorphous  $\text{SiO}_2$   $\epsilon_0 = 3.78$ ),<sup>30</sup>  $\epsilon_{\infty}$  is the high-frequency dielectric constant (for amorphous  $\text{SiO}_2$   $\epsilon_{\infty} = 2.14$ ),<sup>29</sup>  $\epsilon_m$  is the dielectric constant of the surrounding medium, and  $L_k$  are the depolarization factors that depend on the particle shape. Generally, three depolarization factors ( $0 \leq L_k \leq 1$ ) correspond to the three distinct axes of the ellipsoid and satisfy the condition  $L_1 + L_2 + L_3 = 1$ . Although the surrounding medium for small silica particles is air ( $\epsilon_m = 1.0$ ), the effective dielectric constant,  $\tilde{\epsilon}_m$ , is more than unity, because particles are aggregated into globules

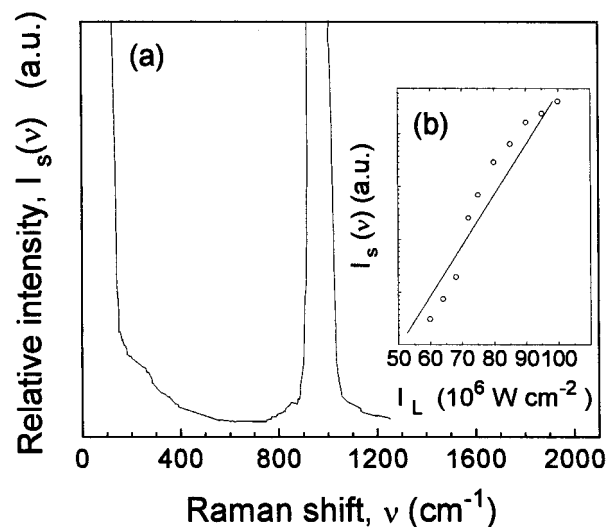


**Figure 4.** SRS spectrum of disperse silica prepared at  $T_{\text{h.t.}} = 600$  °C (a) and the laser intensity dependence of the SRS peak intensity (b). Each point in the inset is averaged over 10 measurements. The straight line indicates the exponential function plotted on the semilogarithmic scale.

of micrometer size.<sup>21</sup> The description of the observed Raman peaks due to SPMs can be made by using the Lorentz profile and eq 1 taking into account that there are six different SPMs corresponding to the location of elliptical particles in two mediums of different effective dielectric constants. The Raman peaks due to SPMs are located at  $909$ ,  $936$ , and  $957\text{ cm}^{-1}$  ( $\tilde{\epsilon}_m^{(1)}$ ) and  $918$ ,  $946$ , and  $966\text{ cm}^{-1}$  ( $\tilde{\epsilon}_m^{(2)}$ ). As shown in Figure 2, good agreement with theory is observed. The following parameters were evaluated:  $L_1 = 0.34$ ,  $L_2 = 0.25$ ,  $L_3 = 0.41$ ,  $\tilde{\epsilon}_m^{(1)} = 1.67$ , and  $\tilde{\epsilon}_m^{(2)} = 1.46$ . Since the dielectric constant of the bulk silica is larger than unity, it is not surprising that the resulting effective dielectric constant is larger than the dielectric constant of air.

Note that the aforementioned Raman peaks corresponding to the SPMs satisfy all requirements that were discussed in the Introduction except for the first one. So, these peaks are located between the  $\text{TO}_2$  and  $\text{LO}_2$  phonon frequencies and shifted to lower frequencies as the effective dielectric constant of the aggregate increases. Also, these Raman peaks are particularly polarized. From our viewpoint, the first requirement has a limited application. Really, the intensity of the Raman peaks due to the SPM cannot increase constantly as the particle size decreases. Evidently, the excitation of SPMs would be impossible in certain sizes of particles approaching the lattice constant. Therefore, this requirement may not be obeyed by very small particles of nanometer size.

## Conclusions

In conclusion, the current work demonstrates the following new phenomena for aggregated silica nanoparticles: (i) the SPMs located between  $\text{TO}_2$ – $\text{LO}_2$  bending phonon modes can be detected by using Raman spectroscopy; (ii) these modes indicate the elliptical shape of silica nanoparticles and can be excited in stimulated processes; (iii) the formation of the bulk crystalline structure from amorphous  $\text{SiO}_2$  nanoparticles can be observed at  $T_{\text{h.t.}} \sim 1000$  °C.

**Acknowledgment.** A partial support of this work by the American National Research Council is acknowledged.

## References and Notes

- (1) Inokuma, T.; Arai, T.; Ishikawa, M. *Phys. Rev. B* **1990**, *42*, 11093.

- (2) Borrelli, N. F.; Hall, D. W.; Holland, H. J.; Smith, D. W. *J. Appl. Phys.* **1987**, *61*, 5399.
- (3) Zheng, J. P.; Kwok, H. S. *Appl. Phys. Lett.* **1989**, *54*, 1.
- (4) Tanaka, A.; Onari, S.; Arai, T. *Phys. Rev. B* **1993**, *47*, 1237.
- (5) Saenger, D. U. *Phys. Rev. B* **1996**, *54*, 14604.
- (6) Kuzmany, H.; Winkler, R.; Pichler, T. *J. Phys.: Condens. Matter* **1995**, *7*, 6601.
- (7) Dresselhaus, M. S.; Dresselhaus, G.; Eklund, P. C. *Science of Fullerenes and Carbon Nanotubes*; Academic Press: New York, 1996.
- (8) Hinra, H.; Ebbesen, T. W.; Tanigaki, K.; Takahashi, H. *Chem. Phys. Lett.* **1993**, *202*, 509.
- (9) Holden, J. M.; Zhou, Ping; Bi, Xiang-Xin; Eklund, P. C.; Bandow, Shunji; Jishi, R. A.; Das Chowdhury, K.; Dresselhaus, G.; Dresselhaus, M. S. *Chem. Phys. Lett.* **1994**, *220*, 186.
- (10) Eklund, P. C.; Holden, J. M.; Jishi, R. A. *Carbon* **1995**, *33*, 959.
- (11) Rao, A. M.; Richter, E.; Bandow, Shunji; Chase, Bruce; Eklund, P. C.; Williams, K. A.; Fang, S.; Subbaswamy, K. R.; Menon, M.; Thess, A.; Smalley, R. E.; Dresselhaus, G.; Dresselhaus M. S. *Science* **1997**, *275*, 187.
- (12) Bohren, C. F.; Huffman, D. R. *Appl. Opt.* **1981**, *20*, 959; *Absorption and scattering of light by small particles*; Wiley: New York, 1983.
- (13) Bockelmann, H. K.; Schlecht, R. G. *Phys. Rev. B* **1974**, *10*, 5225.
- (14) Vijayalakshmi, S.; George, M. A.; Grebel, H. *Appl. Phys. Lett.* **1997**, *70*, 708.
- (15) Rupp, S.; Quilty, J.; Trodahl, H. J.; Ludwig, M. H.; Hummel, R. E. *Appl. Phys. Lett.* **1997**, *70*, 723.
- (16) El-Shall, M. S.; Li, S.; Turkki T.; Graver, D.; Pernisz, U. C.; Daraton, M. I. *J. Phys. Chem.* **1995**, *99*, 17805.
- (17) Li, S.; Silvers, S. J.; El-Shall, M. S. *J. Phys. Chem.* **1997**, *101*, 1794.
- (18) Rupp, R.; Englman, R. *Rep. Prog. Phys.* **1970**, *33*, 144.
- (19) Martin, T. R.; Genzel, L. *Phys. Rev. B* **1973**, *8*, 1630.
- (20) Hayashi, S.; Kanamori, H. *Phys. Rev. B* **1982**, *26*, 7079.
- (21) Gorlov, Yu. I.; Chuiko, A. A. *Surface Chemistry of Silica: Surface Structure, Active Centers, Sorption Mechanisms*; Naukova Dumka: Kiev, 1992 (in Russian).
- (22) Galeener, F. L.; Lucovsky, G. *Phys. Rev. Lett.* **1976**, *37*, 1474.
- (23) Montero, I.; Galan, L.; Najmi, O.; Albella, J. M. *Phys. Rev. B* **1994**, *50*, 4881.
- (24) Wilson, M.; Madden, P. A.; Hemmati, M.; Austen Angell, C. *Phys. Rev. Lett.* **1996**, *77*, 4023.
- (25) Kirk, C. T. *Phys. Rev. B* **1988**, *38*, 1255.
- (26) Carpenter, J. M.; Price, D. L. *Phys. Rev. Lett.* **1985**, *54*, 441.
- (27) Bell, R. J. *Rep. Prog. Phys.* **1972**, *35*, 1315.
- (28) Belyak, Yu. N.; Glinka, Yu. D.; Krut', A. V.; Naumenko, S. N.; Ogenko, V. M.; Chuiko, A. A. *Zh. Prikl. Spektrosk.* **1993**, *59*, 77 [*J. Appl. Spectrosc.* **1993**, *59*, 515].
- (29) Shapiro, S. M.; O'Shea, D. C.; Cummins, H. Z. *Phys. Rev. Lett.* **1967**, *19*, 361.
- (30) Silin, A. R.; Trukhin, A. N. *Point Defects and Elementary Excitation in Crystalline and Glassy SiO<sub>2</sub>*; Zinatne: Riga, 1985 (in Russian).